JOURNAL OF CATALYSIS 94, 491–500 (1985)

Characterization of Crystalline Zirconium Phosphates and Their Isomerization Activities

KOH-ICHI SEGAWA,[1] YASUHIKO KURUSU, YASUO NAKAJIMA, AND MAKIO KINOSHITA

Department of Chemistry, Faculty of Science and Technology, Sophia University, 7-1 Kioicho Chiyoda-ku Tokyo 102, Japan

Received December 6, 1984; revised February 22, 1985

The catalytic activities for ring-opening isomerization of cyclopropane and isomerization of butenes have been examined on crystalline zirconium phosphates. ε-$Zr(HPO_4)_2$ catalyst was highly crystallized during the dehydration of zirconium phosphate gel with concentrated phosphoric acid solution under reduced pressure. This catalyst, which was evacuated at higher temperatures (above 770 K), exhibited higher catalytic activities (based on unit surface area) than α-$Zr(HPO_4)_2 \cdot H_2O$ catalyst or other conventional solid acid catalysts. The coisomerization of d_0- and d_8-1-butene suggests that isomerization would proceed on protonic acid sites even after heat treatment at 1100 K. After evacuation at 773 K, most of phosphate groups were removed, with consequent loss of water, due to the condensation of phosphate groups between each zirconium atom layer. However, a trace amount of residual phosphate groups still remained on the surface. After heat treatment at higher temperatures, the stretching and bending vibration of P–O–P appeared in infrared studies; their intensities increased with increasing temperatures of evacuation. Even though the protonic concentrations decreased, the reaction rates for isomerization were drastically enhanced, because of the presence of P–O–P bonds which could withdraw the electrons from the residual phosphate groups on the surface. Thus some enhancement of acid strength of protons of phosphate groups may occur.

INTRODUCTION

Several kinds of layered compounds have been offered for use as catalysts; these include silicate, graphite, transition metal dichalcogenites, metal chloride oxides, and zirconium phosphate. The distinct features of layered compounds are that the forces holding the layers together are van der Waals forces and electrostatic potentials (*1*). Those materials can be expected to provide new application of catalysts.

The most extensively investigated crystalline zirconium phosphate is an α-layered acid salt, zirconium bis(monohydrogen orthophosphate), which is usually obtained as the monohydrated form. But only a few workers (*2–4*) have reported this to be a solid acid catalyst. α-$Zr(HPO_4)_2 \cdot H_2O$ (abbreviated as α-ZrP) crystallizes in the monoclinic system, as assigned by Clearfield (*5*). Each layer consists of planes of zirconium atoms bridged through phosphate groups which alternate above and below metal atom planes. The proton of the phosphate group can be replaced by another cation without any alteration in the structure of the layer itself (*6*). Thus, each layer may be considered a planar macroanion $[Zr_n(PO_4)_{2n}]^{2n-}$, whose negatively charged oxygens are balanced by an equivalent amount of protons or other cations. Between each layer there are cavities. In the case of α-ZrP, these cavities are filled with water of crystallization, and are stabilized by hydrogen bonding between phosphate groups.

We could prepare highly crystalline ε-$Zr(HPO_4)_2$ (abbreviated as ε-ZrP), which is supposed to have a more simple structure than α-ZrP, since it has no water of crystallization. Therefore, the distances between zirconium atom layers are smaller than for the α-form. This ε-ZrP showed remarkable

[1] To whom all correspondence should be addressed.

0021-9517/85 $3.00

catalytic activities (based on unit surface area) for the isomerization of cyclopropane and butenes, by comparison with α-ZrP and other conventional solid acids (*7*). The present work has been done to study the structures of ε-ZrP after calcination at various temperatures and to compare them with the catalytic activities for some specific surfaces.

EXPERIMENTAL

Preparation of crystalline zirconium phosphate. Zirconium phosphate gel (abbreviated as ZrP-gel) was obtained by the addition of a soluble Zr(IV) salt to phosphoric acids, which results in the precipitation of a gelatinous, amorphous solid of variable composition (*8*). The stoichiometric crystalline compound can be prepared by refluxing these gels in concentrated phosphoric acid (*8*). For the preparation of ε-ZrP, a higher concentration of phosphoric acid is required (*9*) than in the case of α-ZrP. However, the procedure in detail is not clear. Finally, during the removal of the hydrated water (part of which is water of crystallization) of ZrP-gel by refluxing with phosphoric acid, ε-ZrP crystallized in various ways, depending on the temperature and the process time, for a specific concentration of phosphoric acid. In order to complete the dehydration process, we heated the ZrP-gel with concentrated phosphoric acid under reduced pressure. By this procedure, highly crystalline ε-ZrP has been obtained in a shorter process time. The procedure has been described in detail elsewhere (*7*). α-ZrP was obtained by the method of Clearfield (*8*). In brief, ZrP-gel was refluxed with phosphoric acid (10 mol · dm^{-3}) for 50 h. The resulting crystals were washed and dried at room temperature under reduced pressure.

Thermal analysis. Both thermal gravimetric analysis (TGA) and temperature-programmed decomposition (TPDE) experiments were performed under vacuum conditions. About 100 mg of a sample was charged in a quartz basket attached to a standard vacuum system (1×10^{-4} Pa). A McBain-type quartz spiral spring was hung down to the sample basket. The weight change during the TGA experiment was determined by the change in length of the spring, which was equipped with a displacement meter (Type 2U, Shinko Electronic). For TPDE examination, the pressure change from the elimination of water molecules during the condensation of phosphate groups was monitored by an ionization gauge (GI-K, ULVAC) which recorded automatically. Both TGA and TPDE experiments were operated simultaneously.

Irreversible adsorbed amounts of NH_3 were measured gravimetrically by using the same electrobalance for TGA at a constant temperature (293°K).

Infrared spectroscopy. A vacuum-tight IR cell having KBr windows was designed to fit an infrared spectrometer (270-30, Hitachi) and to be attached to a vacuum system. Samples (about 5 mg) were dispersed on a thin silicon plate (1 × 2 cm). The cell was arranged so that a sample plate could be lowered into slots between the optical windows for the spectroscopic examination and withdrawn upward by a magnet into a heated portion (self-contained furnace) at various evacuation temperatures.

X-Ray powder diffractometry. X-Ray powder diffraction (XRD) patterns were obtained by diffractometer (Cu$K\alpha_1$, λ = 0.154050 nm; RAD-2A, Rigaku Electronic) after evacuation at a specified temperature of the sample.

Catalytic reactions. Isomerization of 12 kPa of cyclopropane or butenes was carried out at 323–453 K by using a close recirculation system (230 cm^3). Prior to reaction, the catalyst (25–250 mg) was evacuated at a specified temperature. The reaction products were analyzed by a gas chromatograph which was equipped with a 6-m column of VZ-7 at 288 K. The reaction products of coisomerization of d_0- and d_8-1-butene mixture were separated by gas chromatography (VZ-7, 273 K) and subjected to a mass spectrometric analysis. The mass spectrometer

(JMS-D300, JEOL) was usually operated at 15 eV in order to minimize the fragmentation.

RESULTS AND DISCUSSION

Morphology of Zirconium Phosphates

Scanning electron micrographs (SEM) of ZrP-gel (A), α-ZrP (B), and ε-ZrP (C–F) are shown in Fig. 1. The external appearance in each case is different. For α-ZrP (B), the particles exhibit some hexagonal plate-like morphology; the average diameter of the plates is 0.3 μm. This photograph resembles the results reported by Horsley (*10*). In addition, crystals of ε-ZrP (C) are very well formed. The morphology of ε-ZrP also includes hexagonal plates, whose average crystal dimensions are: 4.0 μm in length, 1.0 μm in width, and 0.5 μm in thickness. The shape of these crystals did not change even after evacuation at 523 K (Fig. 1D); this result was also confirmed by XRD examination. However, in (E) and (F) of Fig. 1, the crystals decreased in size by about 10 to 20% after evacuation at higher temperatures (750–1100 K). The constricted crystals gave XRD results which are similar to the patterns of zirconium diphosphate (ZrP_2O_7, pyrophosphate); see Table 1.

TABLE 1

X-ray Diffraction Powder Patterns of ε- and α-Zirconium Phosphate Phases Evacuated at Different Temperatures

ε-$Zr(HPO_4)_2$				α-$Zr(HPO_4)_2 \cdot H_2O$			
473 K		873 K		298 K		823 K	
d (nm)	I/I_0	*d* (nm)	I/I_0	*d* (nm)	I/I_0	*d* (nm)	I/I_0[a]
0.565	100	0.517	20	0.759	64	0.643	4[b]
0.475	5	0.479	15	0.450	40	0.451	9[b]
0.448	39	0.414	100	0.445	23		
0.400	7	0.370	25	0.358	100		
0.390	48	0.351	10	0.353	54		
0.357	22	0.338	15	0.331	5		
0.297	68	0.292	22	0.322	7		
0.282	26	0.266	20	0.265	26	0.266	2[b]
0.270	10	0.249	18	0.263	29		
0.238	10			0.241	9		
0.204	9						

[a] Intensities were normalized by the data (*d*: 0.358, I/I_0: 100) of the sample evacuated at 298 K.
[b] Broad.

Thermal Analysis

The TPDE spectra of ε-ZrP and α-ZrP under vacuum conditions are shown in Fig. 2. The TPDE spectrum of ε-ZrP (A) showed one-stage dehydration due to the condensation of phosphate groups with consequent loss of 1 mol of water (about 6% weight loss). During the evacuation up to 770 K, about 98% of the reaction in Eq. (1) proceeded, as determined by TGA examination, and then the crystal changed to zirconium diphosphate.

$$\varepsilon\text{-}Zr(HPO_4)_2 \xrightarrow{-H_2O\ (590\text{–}700\ K)} ZrP_2O_7(\text{crystal}) \quad (1)$$

$$\alpha\text{-}Zr(HPO_4)_2 \cdot H_2O \underset{+H_2O\ (300\ K)}{\overset{-H_2O\ (350\text{–}500\ K)}{\rightleftharpoons}} \alpha\text{-}Zr(HPO_4)_2 \quad \text{step A}$$

$$\xrightarrow{-H_2O\ (680\text{–}900\ K)} ZrP_2O_7(\text{amorphous}) \quad \text{step B} \quad (2)$$

However, the ε-ZrP (B), which was evacuated at 773 K for 4 h prior to the TPDE experiment, showed a trace amount of water which evolved in the higher temperature region (800–1000 K). These results suggest that about 2% of phosphate groups still remained on the surface even after evacuation at higher temperature. These residual phosphate groups would be on the corners and edges of crystals. For α-ZrP (C in Fig. 2), the TPDE spectrum showed two-stage dehydration due to the elimination of 1 mol of water of crystallization for the lower-temperature peak (step A in Eq. (2)); this step was a reversible reaction when the sample was exposed to water vapor at room temperature. The second stage (step B) is due to the condensation of phosphate groups.

Theoretical derivations (*11*) give Eq. (3) for TPDE experiments:

$$\frac{d\ln(T_m^2/\beta)}{d\ln(1/T_m)} = \frac{E_d}{R}. \quad (3)$$

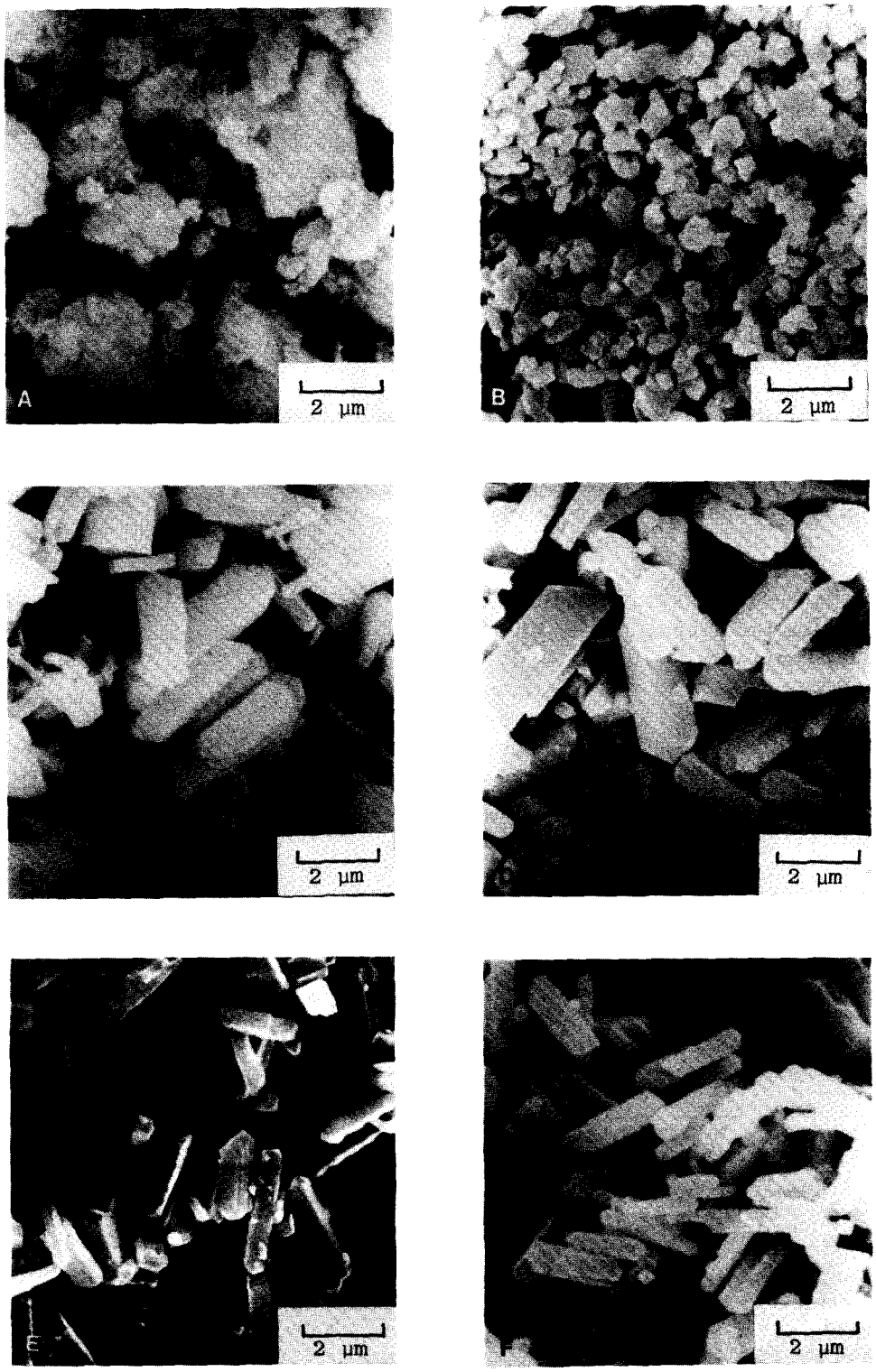

FIG. 1. Scanning electron micrographs of zirconium phosphates: (A) Zirconium phosphate gel, (B) α-$Zr(HPO_4)_2 \cdot H_2O$, (C) ε-$Zr(HPO_4)_2$, (D) ε-$Zr(HPO_4)_2$ evacuated at 523 K, (E) ε-$Zr(HPO_4)_2$ evacuated at 773 K, (F) ε-$Zr(HPO_4)_2$ evacuated at 1100 K.

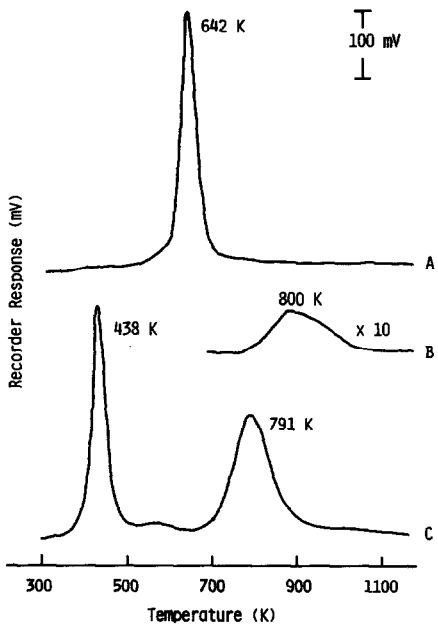

FIG. 2. TPDE spectra of crystalline zirconium phosphates: (A) ε-$Zr(HPO_4)_2$, (B) ε-$Zr(HPO_4)_2$ evacuated at 773 K for 4 h prior to TPDE measurement, (C) α-$Zr(HPO_4)_2 \cdot H_2O$ (heating rate 6.9 K · min^{-1}).

Here T_m is the temperature which corresponds to the maximum rate of decomposition of a sample, β is the heating rate, and E_d is the activation energy for the decomposition. Figure 3 shows the Arrhenius plots for the dehydration of ε- and α-ZrP; these were derived from Eq. (3) at various heating rates (3–10 K · min^{-1}). The slope of ε-ZrP yields activation energies of 133.0 kJ · mol^{-1} for dehydration of crystals due to the condensation of phosphate groups. But for α-ZrP, the slope of lower temperature peak of (C) in Fig. 2, which corresponds to the elimination of water of crystallization, yields lower activation energies (31.8 kJ · mol^{-1}). This number is much lower than the activation energies for the peak of the condensation of phosphate groups (126.0 kJ · mol^{-1}). The results suggest that the waters of crystallization of α-ZrP are held by phosphate groups with hydrogen bonding in each interlayer space; this value seems reasonable, in comparison with other crystalline hydrates (*12*). Besides, within the experimental error, the activation energies of condensation of phosphate groups in each case are almost the same.

Infrared Spectroscopy

The IR spectrum of ε-ZrP evacuated at 298–573 K is shown as (A) in Fig. 4. Four major bands were observed at wavenumbers from 4000 to 600 cm^{-1}. By reference to the IR data of inorganic phosphorus compounds (*13*), these four bands can be assigned as follows: PO–H stretching which gives a band at 3435 cm^{-1}, ionic $P–O^-$ stretching at 1140 cm^{-1} (shoulder), P–O stretching at 1105 cm^{-1}, and P–O–H bending at 910 cm^{-1}. Observed PO–H stretching is about 200–300 cm^{-1} lower than the normal mode of vibrations of H_2O (3756 cm^{-1} for ν_3 and 3653 cm^{-1} for ν_1) in C_{2v} symmetry (*14*). Results suggest that each phosphate group has a hydrogen bonding with another phosphate group between layers. After evacuation at higher temperatures, shown as (B), (C), and (D) in Fig. 4, intensities of PO–H stretching, ionic $P–O^-$ stretching, and P–O–H bending decrease concomitantly. On the other hand, the stretching and bending vibration of P–O–P appeared at 980 and 750 cm^{-1}; their intensities were increased with increasing evacuation temperatures.

The spectrum of α-ZrP, shown as (A) in

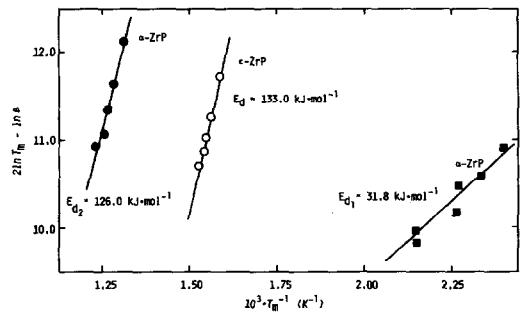

FIG. 3. Arrhenius plots for thermal dehydration of crystalline zirconium phosphates. ○, ε-$Zr(HPO_4)_2$ (condensation of phosphate groups); ■, α-$Zr(HPO_4)_2 \cdot H_2O$ (elimination of water of crystallization); and ●, α-$Zr(HPO_4)_2 \cdot H_2O$ (condensation of phosphate groups).

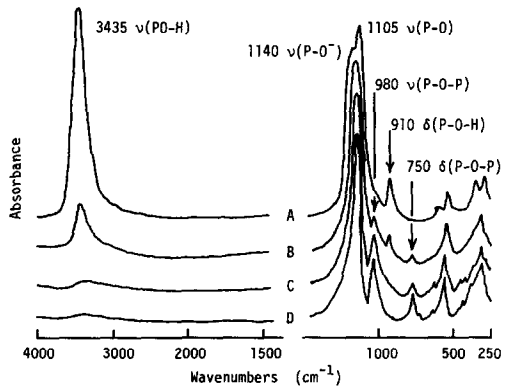

FIG. 4. IR spectra of ε-$Zr(HPO_4)_2$ evacuated at different temperatures: (A) 298–573 K, (B) 623 K, (C) 673 K, (D) 773–1073 K.

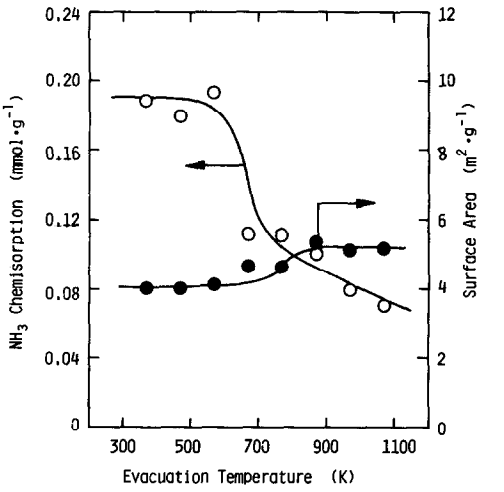

FIG. 6. BET surface area and ammonia chemisorption at 293 K on ε-$Zr(HPO_4)_2$ after evacuation at different temperatures.

Fig. 5, was quite different from ε-ZrP. At the O–H stretching vibration region, there are four bands: one corresponds to the PO–H stretching at 3280 cm^{-1} (*14*); the other three bands, which occur at 3590, 3515, and 3155 cm^{-1}, are attributed to O–H stretching of the water of crystallization in different environments. These three bands are associated with H–O–H bending at 1618 cm^{-1}.

Ammonia Chemisorption

The measurements of NH_3 chemisorption at 293 K on ε-ZrP after evacuation at various temperatures are shown in Fig. 6. The amount of NH_3 chemisorption on ε-ZrP after evacuation below 573 K is about 0.2 mmol · g^{-1}, which contains only about 3% of the original phosphate protons, if we assume one NH_3 molecule interacts with some one phosphate proton. These results suggest that most of NH_3 molecules cannot enter into the interlayer space of ε-ZrP, because of rather narrower layer separation. Besides, after evacuation at higher temperatures (above 650 K), the amount of chemisorption has been decreased by one third. On the other hand, NH_3 and other organic bases easily penetrate into α-ZrP and make some intercalation compounds. For example, uptakes of *n*-butyl amine on α-ZrP are about 6.0 mmol · g^{-1} (*15*), which is a much larger amount of chemisorption than on ε-ZrP.

BET surface areas were almost constant (4–5 m^2 · g^{-1} for ε-ZrP and 11–12 m^2 · g^{-1} for α-ZrP) regardless of evacuation temperature.

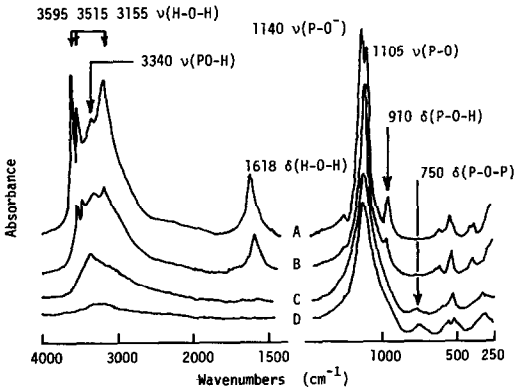

FIG. 5. IR spectra of α-$Zr(HPO_4)_2 \cdot H_2O$ evacuated at different temperatures: (A) 298–373 K, (B) 443–693 K, (C) 700–823 K, (D) 1073 K.

XRD Examination

From the XRD patterns, the structure of ε-ZrP can be assigned to be a layered one, making reference to α-ZrP (*5*). The data of XRD patterns of ε- and α-ZrP have been summarized in Table 1. All phosphate groups are directed toward the interlayer space above and below zirconium atom

planes. The layer separation of zirconium atom planes is about 0.56 nm, which is about 0.2 nm smaller than α-ZrP. When the crystals were evacuated at higher temperatures (700–1100 K), the ε-ZrP XRD peaks quickly changed to patterns similar to cubic zirconium diphosphate (pyrophosphate), and the distance of zirconium atom plane was also changed to 0.52 nm. As was stated previously, a trace amount of residual phosphate groups still remained on the surface at those evacuation temperatures, even though the XRD patterns are quite similar to zirconium diphosphate.

On the other hand, the thermal stabilities of α-ZrP are less than those of ε-ZrP. α-ZrP after evacuation at 500 K, whose chemical composition is equivalent to ε-ZrP (see step A in Eq. (2)), did not have the same crystal structure as ε-ZrP. In addition, the crystals eventually became amorphous materials at higher evacuation temperatures.

Catalytic Reactions

Isomerization of cyclopropane. The ring opening isomerization of cyclopropane is known to be catalyzed by protonic acid sites (*16, 17*). The reaction rate at 453 K and apparent activation energies for isomerization of cyclopropane were measured. On ε-ZrP evacuated at 523 K, the reaction rate was 3.9×10^{-9} $s^{-1} \cdot m^{-2}$, while on the catalyst evacuated at 773 K the value (3.1×10^{-7} $s^{-1} \cdot m^{-2}$) was much higher. However, the values of the activation energies (~60 $kJ \cdot mol^{-1}$) for this reaction are independent of the evacuation temperature within the experimental error. The catalyst evacuated at 773 K has a much smaller number of phosphate groups than the catalyst evacuated at 523 K. It is quite interesting that, no matter how small the protonic concentrations become, the reaction rate for isomerization was enhanced and became about 80 times faster than on the catalyst evacuated at lower temperatures (373–573 K).

Isomerization of butenes. For the isomerization of 1-butene, the ε-ZrP which was evacuated at 773°K showed higher catalytic activities than those of other forms of zirconium phosphates such as α-ZrP and ZrP-gel, or other conventional solid acids, such as alumina (JRC-ALO-4) and silica–alumina (JRC-SAL-2) based on unit surface area (*7*). For ε-ZrP catalyst, the activities and selectivities for isomerization are drastically changed from below to above the boundary of evacuation temperatures at 680 K; these values are shown in Fig. 7. Activities were enhanced by three orders of magnitude at higher evacuation temperature (773 K). And selectivity of product *cis/trans* ratio of 2-butene was changed from 2 to 1 from before to after evacuation at 650 K. At this evacuation temperature, about 90% of the phosphate groups has been removed from the original ε-ZrP; these results are in good agreement with TPDE data in Fig. 2. Furthermore, the reactions of butenes such as *cis*- and *trans*-2-butenes showed the similar temperature dependencies on evacuation. Thus a similar reaction mechanism of isomerization can be predicted for all butenes. In comparison with α-ZrP in Fig. 8, the catalytic activity of ε-ZrP after evacuation at 773 K was about 800 times higher than that of α-ZrP. During

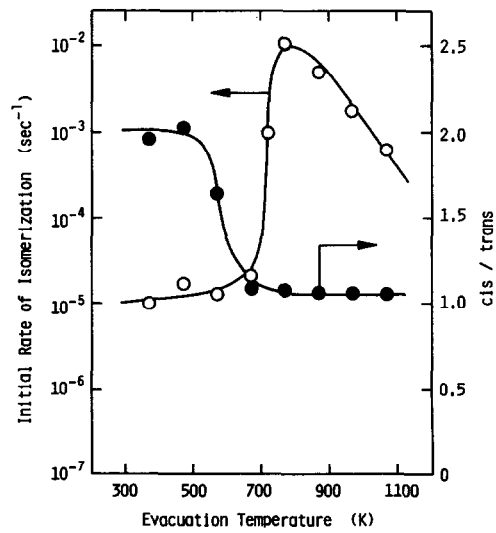

FIG. 7. Isomerization of 1-butene on ε-$Zr(HPO_4)_2$ after evacuation at different temperatures (reaction temperature 353 K).

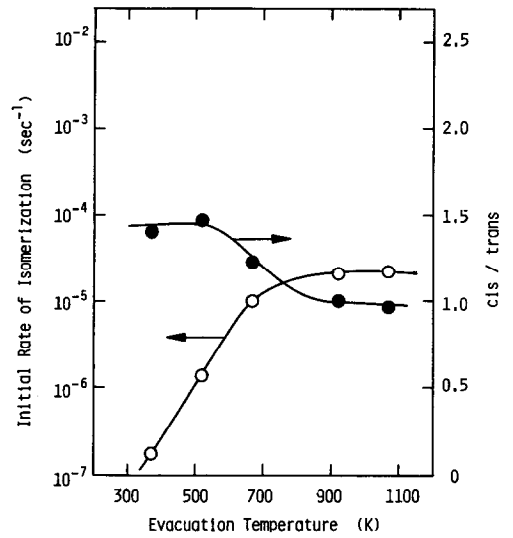

FIG. 8. Isomerization of 1-butene on α-$Zr(HPO_4)_2 \cdot H_2O$ after evacuation at different temperatures (reaction temperature 353 K).

the heat treatment of α-ZrP above 700 K, the crystals changed into amorphous materials (see Table 1), which suggests that the condensation of phosphate groups may be occurring randomly. That will be the reason why α-ZrP and ZrP-gel have lower catalytic activities than ε-ZrP, since the formation of P–O–P bonds might affect the acid properties of crystal.

The product ratios of *cis/trans* of 2-butenes from 1-butene isomerization, which were obtained by extrapolating to zero conversion, became 1 on the ε-ZrP catalyst evacuated above 670 K (see Fig. 7). These results, together with the result of the reaction of cyclopropane (Table 2), strongly suggest the presence of protonic acid sites on the surface. In order to confirm the role of protonic acid sites on ε-ZrP which was evacuated at 773 K, coisomerization of equimolecular d_0- and d_8-1-butene has been examined; the results appear in Fig. 9. The number of H (or D) atoms exchanged per molecule (AEM value) and isotopic effect (IE value) were calculated with the method by Hall and Hightower (*18*). The major species in the initial products of 2-butenes were d_0- and d_7-2-butenes; these were followed by the products of d_1- and d_8-2-butenes. Neither *cis/trans* ratio nor *d* distribution changed at conversions up to 40%.

TABLE 2

Ring Opening Isomerization of Cyclopropane on ε-$Zr(HPO_4)_2$ Evacuated at Different Temperatures

Evacuation temperature (K)	Reaction rate[a] (10^{-10} $s^{-1} \cdot m^{-1}$)	Activation energy (kJ · mol^{-1})
523	39	54
773	3100	69

[a] Initial rate of isomerization.

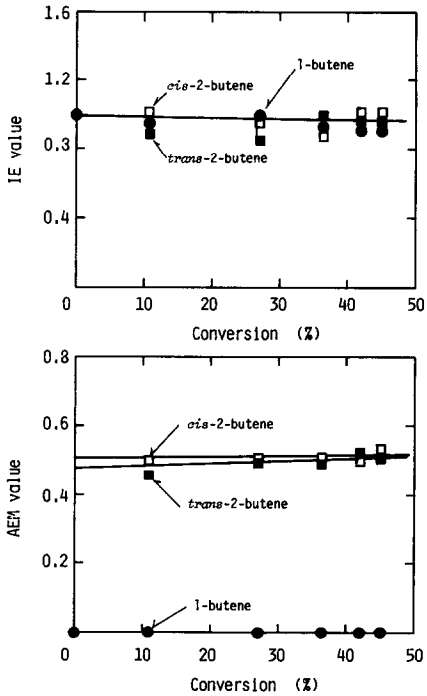

FIG. 9. Coisomerization of d_0- and d_8-1-butene (1/1) on ε-$Zr(HPO_4)_2$ evacuated at 773 K: (A) IE value, isotope effect; (B) AEM value, number of H (or D) atoms exchanged per molecule (reaction temperature 353 K).

$$\mathrm{IE} = \left(\sum_{i=0}^{3} N_i + 0.5N_4\right) \Big/ \left(\sum_{i=5}^{8} N_i + 0.5N_4\right)$$

$$\mathrm{AEM} = \sum_{i=0}^{4} i \cdot N_i + \sum_{i=5}^{8} (8 - i) \cdot N_i.$$

N_i is the fraction of isotopic species containing *i*D atoms; see Ref. (*18*).

Besides, no d_2- to d_6-2-butenes have been observed at this conversion. Only small isotopic effects in Fig. 9 have been observed, which indicates that C–H bond cleavage is not involved in the rate-determining step. The intercept of AEM value in Fig. 9 gave a value near 0.5 for product 2-butenes. The unreacted 1-butene did not exchange its H or D atom during the reaction. These results strongly suggest that one H (or D) atom is exchanged intermolecularly per molecule isomerized, and the reaction would proceed as a typical Brønsted acid-catalyzed reaction.

The time courses for isomerization of butenes on ε-ZrP showed the typical acid-catalyzed reactions for all butenes; this resembles the results for silica–alumina (*19*). Reaction rates obeyed good first-order kinetics; the rate constant of isomerization for each butene agreed with Eq. (4) after evacuation of ε-ZrP at both lower and higher temperatures (300–1100 K):

$$(k_{c1} \cdot k_{1t} \cdot k_{tc})/(k_{1c} \cdot k_{ct} \cdot k_{t1}) = 1. \quad (4)$$

Here, for example, k_{c1} is the rate constant for isomerization of *cis*-2-butene to 1-butene. These results suggest that isomerization of butenes is a three-component kinetic system with competitive reversible reactions (*20*).

Two distinctive reaction mechanisms for butenes can be proposed on ε-ZrP catalyst: which one occurs depends on the temperature of evacuation. For the catalyst evacuated at lower temperatures (300–600 K), the initial *cis/trans* ratio of the reaction of 1-butene was about 2; the reaction proceeds on the terminal phosphate group and oxygen atom are attached to the same phosphorous atom at the same time in a concerted mechanism (switch mechanism). Since the ratio of statistical concentration of *gauche*- and *anti*-1-butene is 2 to 1 (*21*), the selectivity of reaction should affect by this ratio. Those active sites would be on the surface of crystals. For the catalyst evacuated at higher temperatures (700–1100 K), the catalytic activities are higher than in the former case, but the initial *cis/trans* ratio was 1; the reaction proceeds on the proton of the residual phosphate groups. In this case, the reaction intermediates of isomerization of 1-butene would be common secondary butyl carbenium ions (*19*).

Recently, Clearfield and Frianeza (*22*) reported the catalytic activity for dehydration of cyclohexanol on crystalline titanium phosphate and mixed titanium–zirconium phosphates. They concluded that the enhancement of activities after calcination at higher temperatures (above 673 K) was due to the regeneration of phosphate groups with water molecules which evolved during the dehydration reaction. The regeneration of phosphate groups could occur either on Lewis acid sites or on imperfectly formed pyrophosphate groups. However, this interpretation cannot apply for a nonaqueous system. In addition, when ε-ZrP catalyst was treated with a small amount of water vapor prior to reaction, a drastic retardation of activity for isomerization of butene or cyclopropane has been observed. The results of IR measurements show that ε-ZrP has hydrogen bondings with each phosphate group located between zirconium atom planes. Butenes or cyclopropane would be able to adsorb and react on the surface active sites, but not on phosphate protons in the interlayer space, because of smaller layer separations and the presence of hydrogen bondings. But on the catalysts after evacuation at higher temperatures, IR results indicate the presence of P–O–P bonds, which may enhance the protonic character of the residual phosphate groups; those are located only on the crystal surfaces. P–O–P bonds could withdraw the electrons from the residual phosphate protons. In this case, the catalytic activities for isomerization of butenes and cyclopropane would become much higher than original ε-ZrP.

REFERENCES

1. Alberti, G., and Castantino, U., *in* "Intercalation Chemistry" (M. S. Whittingham and A. J. Jacob-

son, Eds.), p. 147. Academic Press, New York, 1982.
2. Hattori, T., Ishiguro, A., and Murakami, Y., *Nippon Kagaku Kaishi,* 761 (1977).
3. Clearfield, A., and Thakur, D. S., *J. Catal.* **65,** 185 (1980).
4. Thakur, D. S., and Clearfield, A., *J. Catal.* **69,** 230 (1981).
5. Troup, J. M., and Clearfield, A., *Inorg. Chem.* **16,** 3311 (1977).
6. Alberti, G., *Acc. Chem. Res.* **11,** 163 (1978).
7. Segawa, K., Kurusu, Y., and Kinoshita, M., *in* "Catalysis by Acids and Bases" (B. Imerik, Ed.), Studies in Surface Science and Catalysis Series, p. 183. Elsevier, Amsterdam, 1985.
8. Clearfield, A., and Stynes, J. A., *J. Inorg. Nucl. Chem.* **26,** 117 (1964).
9. Clearfield, A., Landis, A. L., Media, A. S., and Troup, J. M., *J. Inorg. Nucl. Chem.* **35,** 1099 (1973).
10. Horsley, S. E., and Nowell, D. V., *J. Appl. Chem. Biotechnol.* **23,** 215 (1973).
11. Gentry, J., Hurst, N. W., and Jones, A., *J. Chem. Soc. Faraday Trans. 1,* 1688 (1979).
12. Brink, G., and Falk, M., *Canad. J. Chem.* **48,** 2096 (1970).
13. Corbridge, D. E. C., and Lowe, E. J., *J. Chem. Soc.,* 493 (1954).
14. Horsley, S. E., Nowell, D. V., and Stewart, D. T., *Spectrochim. Acta Part A* **30,** 535 (1974).
15. Hattori, T., Ishiguro, A., and Murakami, Y., *J. Inorg. Nucl. Chem.* **40,** 1107 (1978).
16. Hightower, J. W., and Hall, W. K., *J. Phys. Chem.* **72,** 4555 (1968).
17. Kayo, A., Yamaguchi, T., and Tanabe, K., *J. Catal.* **83,** 99 (1983).
18. Hightower, J. W., and Hall, W. K., *Chem. Eng. Prog.* **63,** 122 (1967).
19. Hightower, J. W., and Hall, W. K., *J. Phys. Chem.* **71,** 104 (1967).
20. Haag, W. O., and Pines, H., *J. Amer. Chem. Soc.* **82,** 2488 (1960).
21. Medema, J., *J. Catal.* **37,** 91 (1975).
22. Frianeza, T. N., and Clearfield, A., *J. Catal.* **85,** 398 (1984).